DOI: 10.13009/EUCASS2019-781

DOI: ADD DOINUMBER HERE

Assessment of the effect of the fuel savings scheme in Formation Flight Planning using Switched Optimal Control Techniques

María Cerezo-Magaña†*, Alberto Olivares, Ernesto Staffetti*
Universidad Rey Juan Carlos
Fuenlabrada, Madrid, Spain
maria.cerezo@urjc.es· alberto.olivares@urjc.es · ernesto.staffetti@urjc.es
†Corresponding author

Abstract

Formation flight for commercial aircraft represents a great promise for several concerns related to the air transport system, such as reducing its environmental impact and increasing its capacity. The formation flight planning problem deals with how to group several flights in formations and to find the aircraft trajectories that optimize the overall direct operating costs. In this paper an interesting aspect of the formation flight planning problem has been studied, the effects of different fuel consumption reductions schemes on the trajectories of the aircraft. A case study with two long-haul flights taking into account the wind forecast has been carried out. Simulation results are reported.

1. Introduction

The predicted high traffic growth rate and the growing concerns associated with climate change and environmental issues are engaging all aviation stakeholders with looking for new solutions. Aviation is pursuing these climate goals through a four-pillar strategy [1] which includes operational measures as those studied in this paper. In 2016 the Carbon Offsetting and Reduction Scheme for International Aviation (CORSIA) was established by the International Civil Aviation Organization (ICAO) to help the sector to achieve its climate targets in the short and medium term by complementing emissions reduction initiatives within the sector. The international standards for the implementation of CORSIA have been adopted as an annex to the Chicago Convention which must be applied from 2019 [2]. These initiatives demonstrate that the aviation sector is committed to advances in technology, operations and infrastructure to continue to reduce the aviation's carbon emissions and formation flight represents a great promise to achieve this objective.

The concept of formation flight arose from the observation of nature where many species of bird fly in formation during their migrations [3]. Further on, the efficiency obtained in flock formations was extended to aircraft formations.

The relative position of two aircraft flying in formation strongly influences the drag reduction, in particular the stream-wise distance, also referred to as longitudinal distance. This distance is usually expressed in terms of wingspans and formations are classified based on its value. In formations at short longitudinal distances between aircraft, called close formations in the literature, the aircraft are longitudinally spaced less than 10 wingspans. These formations provide the greatest benefits in terms of drag reduction. In the formations at greater longitudinal distances, called extended formations, the aircraft are longitudinally spaced between 10 and 40 wingspans [4]. The potential drag reduction is lower, especially in separations of more than 20 wingspans. However, extended formations are intrinsically safer than close formations, an essential factor in civil flights.

One of the most important experimental studies on flight formation has been carried out within the framework of the Surfing Aircraft Vortices for Energy (SAVE) project [5]. The results have been obtained using two Boeing C-17 aircraft at longitudinal distances of between 18 and 70 wingspans, observing fuel savings of up to 11% [6, 7].

In [8] a closed-form solution has been derived for the problem of determining the optimal routes of formation flights having a common origin and different destinations, or vice versa. In this study it is assumed that aircraft follow great circle arcs and the leading aircraft does not deviate from its optimal path. In [9] a formation flight planning framework has been presented. First, a heuristics is developed to identify flights that could potentially benefit from formation flight. Then, all the possible partitions of the set of selected flights into subsets formed by up to three elements are

DOI: 10.13009/EUCASS2019-781

generated. Hence, the subsets of the partition are individually optimized for minimum cost or fuel burn in which the design variables are the merging and splitting points of the routes represented by great circle arcs. Breguet range equation is used to calculate fuel consumption. Finally, the best partition is selected.

In [10] an analytic-geometric approach is presented. A scalable methodology has been defined to solve this problem which enables efficient calculation of formation costs in which the Breguet range equation is used to calculate fuel consumption and weighting schemes are used to incorporate the effects of the drag reduction arising from formation flight.

These approaches to formation flight planning are based on approximations in the sense that they are essentially geometric methods in which neither the dynamic models of the aircraft nor the meteorological forecast are taken into account. However, in flight planning accurate dynamic modeling of the aircraft is necessary to obtain feasible solutions and wind forecast is crucial to achieve more realistic fuel savings. Therefore, the primary objective of this paper is to present a methodology for formation flight planning which is able to consider all the aspects of the problem, in particular, an accurate model of the system, which is actually an hybrid system, and wind forecast.

In this paper, a novel approach to the formation flight planning problem is presented which is formulated as an optimal control problem for a switched system represented by the joint dynamic behavior of a set of aircraft. In this model, aircraft are assumed to have several flight modes and the discrete state of the switched system is the result of their combination.

To model switching decisions between discrete states of the system the embedding approach has been used [11, 12]. The main advantages of this technique are that integer or binary variables do not have to be introduced to model switching decisions between discrete states and that a multiphase formulation of the problem, which would require to make assumptions about the number of phases, is not necessary. Therefore, the switched optimal control can be solved as a classical optimal control problem. In this paper a pseudospectral approach has been employed to solve the resulting optimal control problem [13].

Additionally, a study of the influence of the fuel savings scheme for the follower aircraft in a two long-haul flights is carried-out to establish the influence of this parameter on the solution, in particular on the overall direct operating cost of the set of flights.

The formation flight planning problem can be stated as follows: given a set of commercial flights together with their departure and arrival locations, their departure timetable, the weather forecast and the fuel savings scheme during formation flight, establish how to group them, in formations or solo flight, and find the trajectories to optimize the overall direct operating costs. In particular, rendezvous and splitting locations and times should be also determined. In this paper the following problem is addressed: how the changes on the fuel burn reduction of the trailing aircraft in the formation affects the solution of a formation flight planning problem?

The paper is divided into several sections addressing different aspects of this work. Section 2 describes the model of the system which has been employed to perform the study of the problem. In Section 3 the methodology used is presented. Finally, simulation results are given and analyzed in Section 4.

2. Model of the system

2.1 Equations of motion

Considering that aircraft will not join in formation during take-off, landing and approach phases of flight [14], a simplified common two-degree-of-freedom dynamic model is considered. A point variable-mass model is assuming for all aircraft in the cruise phase. The motion is restricted to the horizontal plane at the tropopause altitude over an spherical Earth model. A symmetric flight without sideslip has been considered and all the aircraft forces are supposed to be in the plane of symmetry of aircraft. Wind effects has been considered in the baseline scenario. All aspects associated to the rotational dynamics are neglected.

The system of kinematics and dynamics differential-algebraic equations (DAE) of aircraft motion employed can be written as:

DOI: 10.13009/EUCASS2019-781

$$\begin{aligned}
\dot{\phi}(t) &= \frac{V(t)\cdot\cos\chi(t) + V_{W_N}(t)}{R_E + h}\\
\dot{\lambda}(t) &= \frac{V(t)\cdot\sin\chi(t) + V_{W_E}(t)}{\cos\phi(t)\cdot(R_E + h)}\\
\dot{\chi}(t) &= \frac{L(t)\cdot\sin\mu(t)}{V(t)\cdot m(t)}\\
\dot{V}(t) &= \frac{T(t) - D(t)}{m(t)}
\end{aligned}\tag{1}$$

where the state vector is composed of the five variables on the left-hand side in the equations above, which are the two dimensional position latitude and longitude ϕ and λ, respectively, the heading angle χ, the true airspeed V, and the mass of the aircraft, m. The control variables are the thrust force T, the lift coefficient C_L, and the bank angle μ.
As usual, the lift force is: $L = qSC_L$, where $q = \frac{1}{2}\rho V^2$ is the dynamic pressure, ρ is the air density and S is the reference wing surface area. The aerodynamic drag force, D, is: $D = qSC_D$, where C_D is the drag coefficient. A parabolic drag polar has been assumed: $C_D = C_{D0} + KC_L^2$, where C_{D0} is the zero-lift drag component and K is the induced drag coefficient. Other parameters and variables include the Earth radius R_E, the gravitational acceleration g and the cruise altitude h. V_{W_E} and V_{W_N} are the velocities of the wind components in East-West and North-South direction, respectively.
The mass flow rate equation must be added to the DAE system above:

$$\dot{m}(t) = -T(t)\cdot\eta(t) \tag{2}$$

where η is the thrust specific fuel consumption. In this study, Eurocontrol's Base of Aircraft Data (BADA), specifically version 3.6 [15], has been used to determine it. In particular for jet engines the following equation applies:

$$\eta(t) = C_{f_1}\left(1 + \frac{V(t)}{C_{f_2}}\right)$$

where C_{f1} and C_{f2} are the empirical thrust specific fuel consumption coefficients.

2.2 Flight envelope

Flight envelope constraints represent the performance limitations for a single aircraft. These constraints make reference to flight altitude, load factor, airspeed and many other different parameters of the aircraft referred. BADA 3.6 has been used to determine the following constraints:

$$\begin{array}{rcl}
V_{min}(t) \leq & V_{CAS}(t) & \leq V_{MO},\\
m_{min} \leq & m(t) & \leq m_{max},\\
 & M(t) & \leq M_{MO},\\
T_{min}(t) \leq & T(t) & \leq T_{max}(t),\\
C_{Lmax} \leq & C_L(t) & \leq C_{Lmax},\\
 & |\dot{V}(t)| & \leq a_{lmax}(t),\\
-\mu_{max} \leq & \mu(t) & \leq \mu_{max}
\end{array}\tag{3}$$

where V_{CAS} is the calibrated airspeed which can be calculated as a function of V_{TAS} [15]. V_{min} and V_{MO} are the minimum and maximum operating calibrated speeds, respectively. m_{min} and m_{max} are the minimum and maximum aircraft mass, respectively. M is the Mach number and M_{MO} is the maximum operating Mach number. T_{min} and T_{max} are the minimum and maximum available engine thrust, respectively. C_{Lmin} and C_{Lmax} are the minimum and maximum lift coefficients, respectively. a_{lmax} is the maximum longitudinal acceleration for civil flights. And finally, μ_{max} is the maximum bank angle set by the Air Navigation regulations for passengers comfort in civil flight.
Furthermore, BADA model has some particular equations for the maximum or minimum parameters which are briefly reviewed. $V_{min}(t) = C_{V_{min}}\cdot V_s(t)$ where $C_{V_{min}}$ is the minimum speed coefficient in all flight phases excluding take off, and V_s is the stall speed at each time.
For turbofan propelled aircraft, assuming standard atmosphere conditions, the maximum thrust is defined with the following empirical expression:

$$T_{max}(t) = C_{T_{cr}}\cdot C_{T_{C,1}}\cdot\left[1 - \frac{H_p(t)}{C_{T_{C,2}}} + C_{T_{C,3}}\cdot H_p^2(t)\right]$$

DOI: 10.13009/EUCASS2019-781

where $C_{T_{cr}}$ is the maximum cruise thrust coefficient. $C_{T_{C,1}}$, $C_{T_{C,2}}$ and $C_{T_{C,3}}$ are empirical thrust coefficients and H_p is the geopotential pressure altitude.

2.3 Wind model

ERA-Interim [16] is a third-generation global atmospheric reanalysis. This large dataset provides estimates of a wide variety of atmospheric and surface parameters such as air temperature, pressure and wind at different altitudes and sea-surface temperature. In this study, the authors have used the Eastward and Northward wind speed directions for a specific day and time at a pressure level of 200 hPa.
Given a set of known input data, a function approximation can be obtained constructing a linear space which depends on the relative position with respect to the known data point according to an arbitrary distance measure. This technique is called Radial Basis Function (RBF) [17]. RBFs have the following mathematical representation:

$$F(x) = c_a + c_b x + \sum_{i=0}^{N-1} c_c \Phi(\| x - R_i \|),$$

where x is the input data vector, $F(x)$ is the function approximation, c_a, c_b and c_c are constant coefficients calculated by RBF method, Φ is the basis function of the network and R is a vector containing the centers of the basis functions.
There are different options for the choice of the basis functions. In this work, a Gaussian basis function has been used. Hence, it can be written as:

$$\Phi(x) = exp\left(\frac{-x^2}{2\sigma}\right)$$

where σ is a scaling parameter.
The Eastward and Northward wind speed directions approximated by the RBF method are represented in Fig. 1 and Fig. 2. The selected day is on April 30, 2018, at 12:00.

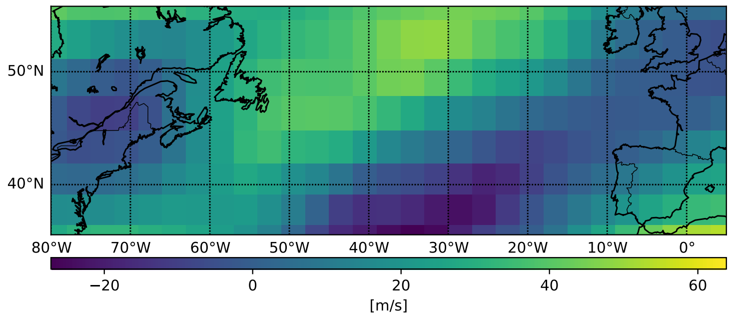

Fig. 1: Eastward wind speed direction on 30 April 2018, 12:00.

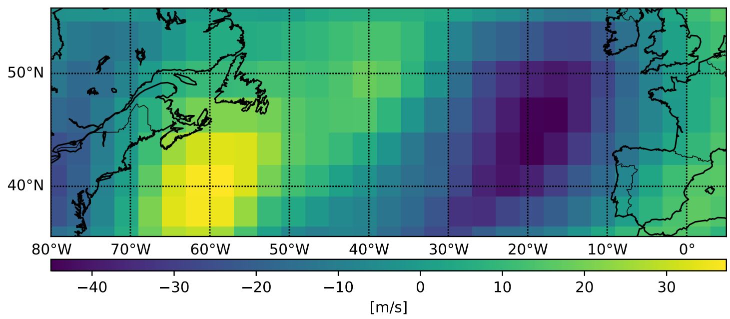

Fig. 2: Northward wind speed direction on 30 April 2018, 12:00.

DOI: 10.13009/EUCASS2019-781

2.4 Formation flight model

The DAE system consisting of Eq. (1) and Eq. (2) are applicable to any aircraft in a cruising phase, only the aircraft parameters will change. But it should be noted that in case of formation, it is necessary to include a modification in Eq. (2) for the trailing aircraft.
As previously mentioned, close formations are unsuitable for commercial flights due to safety reasons. In extended formations the stream-wise distance between aircraft is approximately between 10 and 40 wingspans separation [18]. The authors are agree that beyond 20 spans separation, the potential fuel burn reduction is so smaller. In this conservative work, the maximum spacing to consider formation benefits is 20 wingspans, so beyond it, the formation benefits are considered negligible. Therefore, the formation constraint required to consider fuel burn reduction in the trailing aircraft is the following:

$$10b \leq D \leq 20b \tag{4}$$

For safety reasons the minimum distance between aircraft has been set as $10b$, where b is the leader aircraft wingspread. D is the great-circle distance between two aircraft. Haversine formula has been used to define D.
In the formulation presented, among all feasible formation types, the algorithm should decided which are the optimal ones, including which aircraft will be the leader and the follower. This decision will depend on the type of the aircraft, specially wing span, reference wing area and maximum weight at the rendez-vous point.
The principle of formation flight is based on the fact that any aircraft moving through a fluid generates lift by imparting a swirling motion to the air. This air flow generates downwash and upwash regions. A second aircraft flying in the upwash field created by the first one, will increase its apparent angle of attack obtaining useful energy. The increment of the apparent angle of attack produces an effective rotation of the lift vector resulting in a lower lift-dependent component of drag. So, a significant decrease in drag is achieved [4]. In Fig. 3, a schematic representation of the induced velocity is represented.

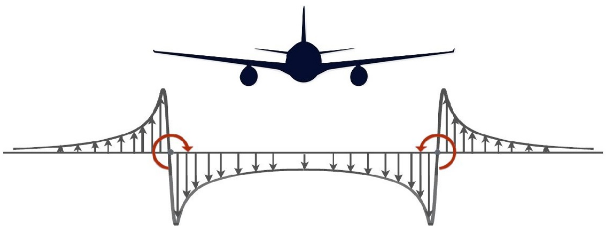

Fig. 3: Vertical component of induced velocity field (not to scale). Figure adapted from [19].

A simplified assumption has been used in this work considering that the reduction in the trailing aircraft induced drag can be modeled directly as a percentage of reduction in fuel burn consumption, $\mathcal{R}_{fuel}$. The fuel saving factor can be directly added in Eq. (2) to get the mass flow rate equation for the trailing aircraft during the formation:

$$\dot{m}_{FF}(t) = -[1 - \mathcal{R}_{fuel}] \cdot T(t) \cdot \eta(t) \tag{5}$$

It is quite difficult to estimate the drag reduction and hence, the fuel burn reduction achieved during a formation flight. There are too many parameters to take into account. The number of aircraft involved in the formation, their model, size and weight, the ability of the follower aircraft to place itself in the optimum location of the wake or the stresses and vibrations induced, among others, strongly influence the benefits of the formation. In this study, a conservative value for the fuel savings scheme for the trailing aircraft of a two aircraft formation is assumed. The maximum adopted value has been a 12% of fuel savings for the trailing aircraft.

2.5 Objective functional

The objective functional is a key factor in all trajectory optimization problems. It is particularly important in optimal formation flight trajectories in which there may be a conflict of interest between the fuel cost and the total mission time. Broadly, the assembling of a formation flight requires that, at least, one of the aircraft involved in the formation changes its solo flight great circle path increasing the flight distance. This detour usually leads to an increase in the total flight time. Besides, it is important to bear in mind that the slower aircraft will determine the maximum velocity of the all aircraft involved in the formation. So, expectedly, formation flight will reduce fuel consumption in the first place and secondly, it will increase the total flight time for the set of aircraft involved in the formation.

DOI: 10.13009/EUCASS2019-781

In this case, the needed to get away from a traditional fuel minimization models arises in order to capture the resultant rise time costs involved. Besides, a maximum deviation of the solo flight time has been set. This means a more realistic problem formulation according to the operational conditions.
Evaluating Direct Operating Costs (DOC) as a whole should include all expenses associated with aircraft flying operations. It is beyond the scope of this work. In the present study, fuel consumption and flight time are only taking into account to define a simplified DOC. Even then, estimating costs related to the increment of the flight time is not straightforward. In [20] a detailed study of the delays cost to airlines is presented. This work intends to provide quantified cost values for the delays. Based on this Eurocontrol report, the penalty coefficients of the objective functional for case study have been chosen. The objective functional for two aircraft states as follows:

$$\min \ \alpha_t \left[t_1 - t_2\right] + \alpha_f \left[f_1 + f_2\right] \tag{6}$$

where α_t and α_m are the time and the fuel burn penalty parameters, respectively, t_1, t_2 and f_1, f_2 are the total flight time and the fuel consumption of each flight, respectively.

3. Solution of the Switched Optimal Control Problem

As said in the introduction, in this paper, a novel approach to the formation flight planning problem is presented which is formulated as an optimal control problem for a switched system represented by the joint dynamic behaviour of a set of aircraft. In this model, aircraft are assumed to have several flight modes and the discrete state of the switched system is the result of their combination. Under these assumptions, the operating modes of the aircraft are the following: solo flight, leader or trailing in a two-aircraft formation. To model switching decisions between discrete states of the system the embedding approach has been used [11, 12]. The main advantages of this technique are that integer or binary variables do not have to be introduced to model switching decisions between discrete states and that a multiphase formulation of the problem, which would require to make assumptions about the number of phases, is not necessary. Not all transition between discrete states are possible at any time, for example, while the distance between aircraft is larger than $20b$, formation flight could not be chosen. Therefore, logical constraints have to be included in the switched optimal control formulation to model the possible discrete state transitions. In general these constraints are in disjunctive form. To introduce logical constraints in disjunctive form in the switched optimal control problem (OCP), the embedding approach has been used [21]. Hence, the switched optimal control can be solved as a classical optimal control problem. This problem is solved using optimal control techniques. The resulting problem is transcribed to a nonlinear programming problem using Pseudospectral Methods (PS). In particular, flipped-Radau Pseudospectral Method [13] has been implemented.
To solve smooth OCP, PS methods are more accurate than the traditional collocation methods [22]. However, using them in solving nonsmooth and hybrid problems, as in this work, can be more complex. The use of global polynomials and predetermined nodes distribution are the key reasons for this complexity. The concept of knots introduced by Ross et al. [23] allows the use of PS methods to hybrid problems such as formation flight. Hence, PS Knotting Methods have been implemented for solving the OCP.
Other important advantage of using this method is that it is easily scalable to formation flight planning problems with an arbitrary number of aircraft and to multiple formation flight planning problems in which aircraft are allowed to leave a formation to join another formation.

4. Numerical Results

In this section, a numerical experiment is presented to demonstrate the effectiveness of the proposed methodology. The experiment involves two transoceanic eastbound flights with the following departure and arrival airports:

- Flight 1: Montreal (YUL) - Barcelona (BCN)
- Flight 2: New York (JFK) - Madrid (MAD)

The aircraft selected for each flight are Airbus A330-200. As mentioned above, in this work only cruise phase has been modeled, the rest of the flight phases are neglected. So, the initial and final cruise phase points for both aircraft have been assumed to be the same as the departure and arrival airports of each flight. The initial mass is assigned, not being equal for both aircraft. The initial and final velocities have been set at typical cruise values for the aircraft model selected. The boundary values for the state variables of each aircraft are listed in Table 1.
Departure times are fixed. The departure time of Flight 1 is at 12:00 and of Flight 2 is 10 minutes later, at 12:10. Arrival times are left free, with a constraint on the maximum temporal deviation from scheduled arrival time for each flight of 30 minutes. The time and fuel burn penalty parameters, α_t and α_m, in Eq. (6) are set to 0.35 and 0.65, respectively.

DOI: 10.13009/EUCASS2019-781

Table 1: Boundary conditions

Symbol	Unit	Airc. 1	Airc. 2
ϕ_I	deg	45.509	40.714
ϕ_F	deg	41.382	40.489
λ_I	deg	-73.588	-74.006
λ_F	deg	2.169	-3.683
χ_I	deg	66.437	66.513
V_I	m/s	240	240
V_F	m/s	220	220
m_I	kg	215 000	220 000

The influence of the fuel saving formation scheme on the solution has been studied. No delays have been considered in order to simplify the study of the effect of the fuel saving scheme. Several numerical simulations have been conducted only changing the fuel saving scheme for the trailing aircraft in a two-aircraft formation. Percentages of fuel saving under 6% are not displayed because flying in formation doesn't optimize the DOC of the mission in the design experiment for those small values of fuel savings. So, the formation won't be chosen by the algorithm for fuel savings smaller than 6%.

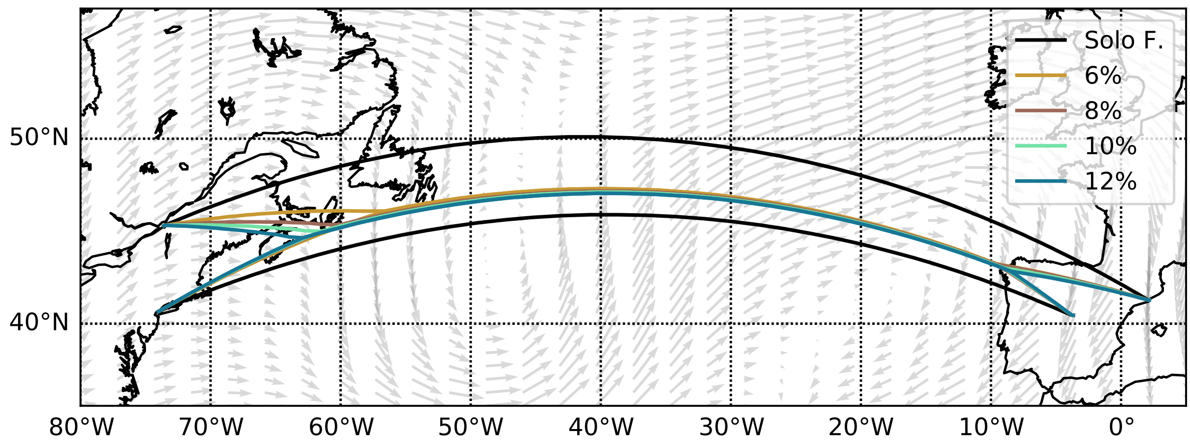

Fig. 4: Comparison of the trajectories of both aircraft for different fuel saving scheme.

The trajectories obtained for the aircraft for different fuel savings percentages are illustrated in Fig. 4. Notice that the scale is not the same for both axis. As mentioned before, for fuel savings smaller than 6% formation flight won't be optimal. Solo flights are represented in black color in the figure. Solo flight trajectories are a bit different from the orthodromic path due to the wind field. Additionally, rendezvous and splitting points differences are illustrated for larger percentages of fuel savings. The larger the fuel savings percentage, the longer is the formation flight. Table 2 summarizes the distances and times of the formation flight phase. There are three different columns for the distance: the total formation flight distance and the percentage of total distance covered for each aircraft. There are three more columns for the time with similar information. It can be observed that for larger fuel burn savings, distance as well as flight time are also larger.

Table 2: Distances and Times of Formation Flight

	Formation Flight Distance			Formation Flight Time		
Fuel Savings [%]	Total [km]	Airc. 1 [%]	Airc. 2 [%]	Total [s]	Airc. 1 [%]	Airc. 2 [%]
6	3724.06	62.36	64.38	15156.42	59.12	63.50
8	3998.10	66.75	69.13	16502.83	64.39	69.12
10	4165.16	69.39	72.02	17217.40	67.16	72.10
12	4314.62	71.70	74.60	17844.23	69.64	74.74

DOI: 10.13009/EUCASS2019-781

The trajectories shown in Fig. 4 also give information about the detour that each aircraft must do to fly in formation. Table 3 synthesizes the extra distance covered by each aircraft comparing it to the solo flight distance. The distance covered has been calculated as a sum of the great circle path between nodes. It is worth mentioning that in every experiment in which formation flight is optimal, Aircraft 1 makes a larger detour than Aircraft 2. This behavior is due to the Jet Stream in the area. The wind velocity of the Jet Stream is represented in Fig. 4 with the grey arrows.

Table 3: Extra distance covered

	Δ Distance [km]		**Δ Distance [%]**		
Fuel Savings [%]	**Airc. 1**	**Airc. 2**	**Airc. 1**	**Airc. 2**	**Total**
6	70.34	17.66	1.18	0.31	1.49
8	88.11	16.60	1.47	0.29	1.76
10	101.17	16.43	1.69	0.28	1.97
12	115.88	16.72	1.93	0.29	2.22

As expected, the results in Table 4 show that for larger fuel savings, the total fuel savings are also larger. Aircraft 1 reduces fuel burn while Aircraft 2 is consuming between 0.42 to 0.46 more fuel than the solo flight. This indicates that Aircraft 1 is the follower and Aircraft 2 is the leader in all the experiments conducted. It results in the need of a cost and benefits sharing scheme to implement formation flight. Finally, in the last column of Table 4 it can be noticed that for different fuel savings scheme, the total fuel burn flying in formation is smaller than the total fuel consumption of the solo flights. A total reduction from 1.64% to 5.47% is achieved for the two flights.

Table 4: Fuel burn consumption

	Fuel Burn [kg]		**Δ Fuel Burn [%]**		
Fuel Savings [%]	**Airc. 1**	**Airc. 2**	**Airc. 1**	**Airc. 2**	**Total**
6	39517.82	40340.01	-2.10	+0.46	-1.64
8	38928.91	40330.01	-3.56	+0.44	-3.12
10	38537.49	40325.61	-4.53	+0.43	-4.10
12	37991.08	40323.27	-5.89	+0.42	-5.47

Fig. 5 illustrates the variation of Mach number of the aircraft for different fuel savings schemes. To help better understand the figure, big points have been used to determine the rendezvous and splitting time for each pair of aircraft. In all the obtained solutions, the distance to the rendezvous point from the departure point is bigger for Aircraft 2 and it has less time to get to it since it is starting 10 minutes later than Aircraft 1. So, Aircraft 2 should cover a bigger distance in less time that's why its velocity needs to be higher than Aircraft 1. In addition, depending on how far the rendezvous point is from departure point of Aircraft 1, this aircraft will decrease its initial velocity to adjust in space and time to meet Aircraft 2 at the optimal rendezvous point and time. It must be pointed out that the Gibbs phenomenon is presented near the rendezvous and the splitting points.

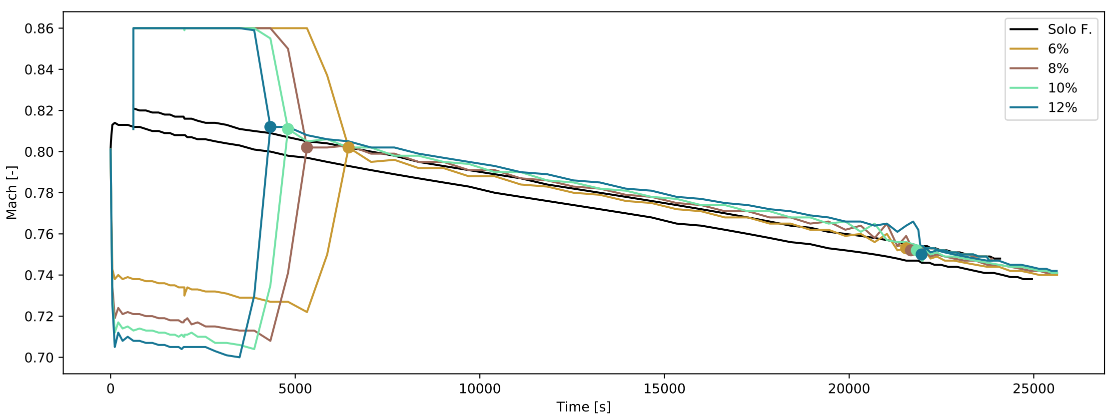

Fig. 5: Comparison of the Mach number of both aircraft for different fuel saving scheme.

DOI: 10.13009/EUCASS2019-781

In Table 5 the total flight time and the increment of the flight time compared to the solo flight time are listed. As seen before in Table 3, both aircraft divert from their solo flight trajectory in order to get the formation. These diversions increase the total flight time of both flights. In the last column of Table 5, a total flight time rise of about 3% is observed for all the different fuel savings schemes. It is remarkable that although for larger fuel savings, the extra distance covered is also larger while the total flight time is not. This is due to the fact that both aircraft vary their velocities in order to get the optimal solution as seen in Fig 5.

Table 5: Total Flight time

	Flight Time [s]		**Δ Flight Time [%]**		
Fuel Savings [%]	**Airc. 1**	**Airc. 2**	**Airc. 1**	**Airc. 2**	**Total**
6	25632.51	23868.11	+2.73	+0.28	+3.01
8	25630.12	23874.14	+2.72	+0.31	+3.03
10	25634.80	23878.28	+2.74	+0.33	+3.07
12	25621.91	23875.48	+2.68	+0.31	+2.99

5. Conclusions

The formation flight has a great potential to contribute to reduce fuel consumption and the environmental impact of the air transport sector and also increase its capacity. The method presented in this paper solves the formation flight planning problem with an accurate modeling of the scenario and carry-out the sensitivity analysis of the solutions to some parameters of the problem. In particular, it has been studied how different fuel saving schemes influence the trajectories of the aircraft flying in formation. These effects have been studied letting all others parameters of the problem fixed. However, there are many other variables affecting the solution, such as the initial mass of the aircraft, delays in departure times of the flights or meteorological conditions. For a more realistic study, the effect of all these parameters should be taken in account in the formation flight planning problem. These aspects will be subject of future research.

6. Acknowledgments

This work has been partially supported by the grants number `TRA2017-91203-EXP` and `RTI2018-098471-B-C33` of the Spanish Government.

References

[1] ICAO, "Environmental report 2016. Aviation and climate change." International Civil Aviation Organization, 2010.

[2] ICAO, "International standards and recommended practices for environmental protection. Annex 16 to the convention on international civil aviation. Volume IV Carbon Offsetting and Reduction Scheme for International Aviation (CORSIA)." International Civil Aviation Organization, 2018.

[3] P. B. S. Lissaman and C. A. Shollenberger, "Formation flight of birds," *Science*, vol. 168, no. 3934, pp. 1003–1005, 1970.

[4] A. Ning, T. C. Flanzer, and I. M. Kroo, "Aerodynamic performance of extended formation flight," *Journal of aircraft*, vol. 48, no. 3, pp. 855–865, 2011.

[5] S. R. Bieniawski, R. W. Clark, S. E. Rosenzweig, and W. E. Blake, "Summary of flight testing and results for the formation flight for aerodynamic benefit program," in *Proceedings of the 52nd Aerospace Sciences Meeting, AIAA SciTech Forum*, 2014.

[6] D. J. Haalas, S. R. Bieniawski, B. Whitehead, T. Flanzer, and W. B. Blake, "Formation flight for aerodynamic benefit simulation development and validation," in *Proceedings of the 52nd Aerospace Sciences Meeting, AIAA SciTech Forum*, 2014.

DOI: 10.13009/EUCASS2019-781

[7] T. C. Flanzer, S. R. Bieniawski, and W. B. Blake, "Operational analysis for the formation flight for aerodynamic benefit program," in *Proceedings of the 52nd Aerospace Sciences Meeting, AIAA SciTech Forum*, (National Harbor, Maryland, USA), 2014.

[8] W. B. Blake and T. C. Flanzer, "Optimal routing for drag-reducing formation flight: A restricted case," *Journal of Guidance, Control, and Dynamics*, vol. 39, no. 1, pp. 173–176, 2016.

[9] J. Xu, S. A. Ning, G. Bower, and I. Kroo, "Aircraft route optimization for formation flight," *Journal of Airfraft*, vol. 51, no. 2, pp. 490–501, 2014.

[10] T. E. Kent and A. G. Richards, "Analytic approach to optimal routing for commercial formation flight," *Journal of Guidance, Control, and Dynamics*, vol. 38, no. 10, pp. 1872–1884, 2015.

[11] S. C. Bengea and R. A. DeCarlo, "Optimal control of switching systems," *Automatica*, vol. 41, pp. 11–27, 2005.

[12] S. Bengea, K. Uthaichana, M. Žefran, and R. A. DeCarlo, "Optimal control of switching systems via embedding into continuous optimal control problem," in *The Control Handbook: Advanced Methods* (W. S. Levine, ed.), ch. 31, pp. 31–1 – 31–23, CRC Press, 2011.

[13] D. Garg, M. A. Patterson, W. Hager, A. V. Rao, D. A. Benson, and G. T. Huntington, "An overview of three pseudospectral methods for the numerical solution of optimal control problems," *Advances in the Astronautical Sciences*, vol. 135, pp. 1–17, 2009.

[14] S. Hartjes, M. E. van Hellenberg Hubar, and H. G. Visser, "Multiple-phase trajectory optimization for formation flight in civil aviation," in *Advances in Aerospace Guidance, Navigation and Control*, pp. 389–405, Springer, 2018.

[15] Eurocontrol, "User manual for the Base of Aircraft Data (BADA)," Tech. Rep. 130416, Eurocontrol, 2013.

[16] D. P. Dee, S. M. Uppala, *et al.*, "The ERA–Interim reanalysis: Configuration and performance of the data assimilation system," *Quarterly Journal of the Royal Meteorological Society*, vol. 137, no. 656, pp. 553–597, 2011.

[17] M. D. Buhmann, *Radial Basis Functions: Theory and Implementations*. Cambridge University Press, 2003.

[18] G. J. Durango, C. Lawson, and A. Z. Shahneh, "Formation flight investigation for highly efficient future civil transport aircraft," *The Aeronautical Journal*, vol. 120, no. 1229, pp. 1081–1100, 2016.

[19] S. A. Ning, *Aircraft Drag Reduction through Extended Formation Flight*. PhD thesis, Stanford University, 2011.

[20] A. J. Cook, G. Tanner, and S. Anderson, "Evaluating the true cost to airlines of one minute of airborne or ground delay," tech. rep., Eurocontrol, 2004.

[21] S. Wei, M. Žefran, and R. A. DeCarlo, "Optimal control of robotic systems with logical constraints: Application to UAV path planning," in *Proceedings of the 2008 IEEE International Conference on Robotics and Automation*, 2008.

[22] J. T. Betts, *Practical methods for optimal control and estimation using nonlinear programming*. SIAM, 2010.

[23] I. M. Ross and F. Fahroo, "Pseudospectral knotting methods for solving optimal control problems," *Journal of Guidance, Control, and Dynamics*, vol. 27, no. 3, pp. 397–405, 2004.